Osteoprogenitor SFRP1 prevents exhaustion of hematopoietic stem cells via PP2A-PR72/130-mediated regulation of p300

Franziska Hettler,[1*] Christina Schreck,[1*] Sandra Romero Marquez,[1] Thomas Engleitner,[2,3] Baiba Vilne,[4,5] Theresa Landspersky,[1] Heike Weidner,[6] Renate Hausinger,[1] Ritu Mishra,[2,7] Rupert Oellinger,[2,3] Martina Rauner,[6] Ronald Naumann,[8] Christian Peschel,[1,9] Florian Bassermann,[1,9] Roland Rad,[2,3,9] Rouzanna Istvanffy[1°#] and Robert A.J. Oostendorp[1#]

[1]Technical University of Munich, School of Medicine, Department of Internal Medicine III Hematology/Oncology, Munich, Germany; [2]Technical University of Munich, School of Medicine, Center for Translational Cancer Research (TranslaTUM), Munich, Germany: [3]Technical University of Munich, School of Medicine, Institute of Molecular Oncology and Functional Genomics, Munich, Germany; [4]Bioinformatics Research Unit, Riga Stradins University Riga, Riga, Latvia; [5]netOmics, Riga, Latvia; [6]Bone Lab Dresden, Department of Medicine III & Center for Healthy Aging, Technische Universität Dresden, Dresden, Germany; [7]School of Medicine, Institute of Clinical Chemistry and Pathobiochemistry, Technical University of Munich, Munich, Germany; [8]Max Planck Institute of Molecular Cell Biology and Genetics, Transgenic Core Facility, Dresden, Germany and [9]German Cancer Consortium (DKTK), Heidelberg, Germany

[°]Current affiliation: Technical University of Munich, School of Medicine, Surgery Department, Munich, Germany

[*]FH and CS contributed equally as co-first authors.
[#]RI and RAJO contributed equally as co-senior authors.

Correspondence: R.A.J. Oostendorp
robert.oostendorp@tum.de

Received: February 2, 2022.
Accepted: August 2, 2022.
Prepublished: August 11, 2022.

https://doi.org/10.3324/haematol.2022.280760

Online supplemental Material

Osteoprogenitor SFRP1 prevents exhaustion of Hematopoietic Stem Cells via PP2A-PR72/130-mediated regulation of p300.

Franziska Hettler[1]*, Christina Schreck[1]*, Sandra Romero Marquez[1], Thomas Engleitner[2,3], Baiba Vilne[4,5], Theresa Landspersky[1], Heike Weidner[6], Renate Hausinger[1], Ritu Mishra[2,7], Rupert Oellinger[2,3], Martina Rauner[6], Roland Naumann[8], Christian Peschel[1,9], Florian Bassermann[1,9], Roland Rad[2,3,9], Rouzanna Istvanffy[1,10], Robert A.J. Oostendorp[1]

Author affiliations:

1. Technical University of Munich, School of Medicine, Department of Internal Medicine III Hematology/Oncology, 81675 Munich, Germany.

2. Technical University of Munich, School of Medicine, Center for Translational Cancer Research (TranslaTUM), 81675 Munich, Germany.

3. Technical University of Munich, School of Medicine, Institute of Molecular Oncology and Functional Genomics, 81675 Munich, Germany

4. Bioinformatics Research Unit, Riga Stradins University Riga, Latvia

5. netOmics, riga, Latvia

6. Bone Lab Dresden, Department of Medicine III & Center for Healthy Aging, Technische Universität Dresden, Dresden, Germany

7. School of Medicine, Institute of Clinical Chemistry and Pathobiochemistry, Technical University of Munich, Munich, Germany.

8. Max Planck Institute of Molecular Cell Biology and Genetics, Transgenic Core Facility, Dresden

9. German Cancer Consortium (DKTK), 69120 Heidelberg, Germany

10. Current address: Technical University of Munich, School of Medicine, Surgery Department, 81675 Munich, Germany

*: These authors contributed equally

Contents page nr.

SupplementaryMethods

Animals and animal models

The *Sfrp1*^{tm1a} mouse line *Sfrp1*$^{fl/fl}$ was generated using EUCOMM *Sfrp1* targeting vector (HTGR03001_Z_2_A0) in C57BL/6N embryonic stem cells (JM8A3.N1, clone HEPD0593_1_C09) [1]. The "knockout first" founder mice expressed FRT-sites flanking a neo cassette, originally present in the targeting conditional potential vector [2]. This cassette was deleted by matings with FLP-*FRT* mice (flippase (FLP) recombinase) [3]. Thereafter, the *Sfrp1* conditional mice (SFRP1^{tm1a} mouse line KO first) were crossed with *OSX1-GFP::Cre* (Osx-Cre; *B6.Cg-Tg(Sp7-tTA,tetO-EGFP/cre)1Amc/J*; Jackson Labs Stock Nr.: 006361) transgenic mice. The Osx1-GFP::Cre transgene carries both tTA under the regulation of the osterix (*Sp7*) promoter and a downstream tetracycline responsive element (TRE; tetO)-controlled GFP/Cre fusion protein. When these transgenic animals are mated to transgenic strains that carry *loxP*-flanked (floxed) conditional alleles, Cre-mediated recombination of the floxed allele in the double mutant animals is placed under the regulation of doxycycline (dox) such that dox administration would prevent fusion protein expression and recombination [4] (Figure 1C). The *loxP* sites are on either side of the critical exon 2 of the *Sfrp1* gene. CRE recombinase deletes exon 2 and induces a frameshift mutation (Figure S1C). The Osx promoter activity is limited to BM osteolineage cells, like (pre-)osteoblasts, osteocytes, and hypertrophic chondrocytes [4]. In addition, progeny of Osx-GFP cells is found in MSPCs, perivascular cells and adipocytes in the bone marrow [5, 6]. Consequently, the deletion of *Sfrp1* in the Osx-Cre conditional mice (OS1Δ/Δ mice) is limited to the mesenchymal stromal cell compartments of the bone marrow.

In all experiments, age- and sex-matched *Sfrp1*$^{+/+}$ (wildtype (WT), *Sfrp1*$^{fl/fl}$ (WT), and *Osx1-GFP::Cre*(WT) littermates were used as controls for comparisons with the OS1Δ/Δ mice.

For the repopulation assays, the F1 crosses of 129S2/SvPasCrl (129; CD45.2; Jackson Labs Stock Nr.: 3587894) and either B6.SJL-Ptprca Pepcb/BoyJCrl (Ly5.1; CD45.1) (129xLy5.1) or C57BL/B6.JCrl (BL6; CD45.2; Jackson Labs Stock Nr.: 2164701) (129xB6) were used as donor or recipient mice unless otherwise specified. These mice were ordered from Charles River Laboratories (Lyon, France, https://www.criver.com) at the age of 6 weeks. The primers for mice genotyping are listed in Supplementary Table 2.

All mice were kept in the Center of Preclinical Research (Zentrum für präklinische Forschung (ZPF)) under specific-pathogen-free (SPF) conditions in micro-isolators in individually ventilated cages (IVC), corresponding to Federation of European Laboratory Animal Science Associations (FELASA) recommendations. All experiments were approved by the Government of Upper Bavaria (Vet_02-14-112, -15-228, and -17-124).

Transplantation assay

For the adult *in vivo* repopulation assay, the CD45 congenic system (CD45.1 and CD45.2) was used to differentiate donor-derived cells and recipient cells and was performed as described previously [7-9]. For transplantation (Tx) 8 to 10-weeks-old, lethally irradiated recipient mice (8.5 Gy) received donor cells via intravenous (i.v.) injection in the tail vein. The transplanted adult mice received 8 mg of the long-term antibiotic Convenia® (80 mg/ml) per kilo of bodyweight via subcutaneous (s.c.) injection. Furthermore, the mice were administered 1 mg/ml Borgal® solution (24%) for a total of three weeks post Tx in drinking water. For the project, 100 sorted Lin$^-$Sca-1 $^+$Kit$^+$CD34$^-$CD150$^+$ donor BM cells (or 1000/2000 sorted LSK donor cells in secondary transplantation assay) of Sfrp1 conditional mice and control mice (CD45.2)

transplanted into 129xLy5.1 (F1; CD45.1xCD45.2), together with 1 x 10^5 BM cells and 5 x 10^5 spleen helper cells from 129Ly5.1 mice. The PB was analyzed in week four, eight, 12, 16, and 20 post Tx by flow cytometry. 20 or 24 weeks after Tx, mice were sacrificed and BM, SP, and PB were analyzed by flow cytometry. Mice were counted positive with ≥ 1% donor engraftment in the myeloid and lymphoid lineage.

Structural and histological bone analysis

To perform bone analyses, long bones and spine were fixed in 4% PFA for 48 hours and then stored in ethanol. Before the measurement, femur length was determined with a digital caliper. Afterward, the bone microarchitecture of femora was analyzed using micro-computed tomography (µCT; vivaCT40, Scanco Medical, Switzerland) with an isotropic voxel size of 10.5 µm (70 kVP; 114 µA, 200 ms integration time). The trabecular bone of femur metaphysis beneath the growth plate was evaluated with 100 slices using established protocols from Scano Medical. To assess the cortical thickness, 100 slices in the middle of the femur were assessed. To investigate the number of osteoclasts as well as osteoblasts per bone perimeter, paraffin-embedded femora were used for tartrate-resistant acid phosphatase (TRAP) staining. For the evaluation of bone parameters, trabecular bone beneath the growth plate in the femora and in the middle of the vertebrae was analyzed using the Osteomeasure software. Pictures were taken with the CellSens program. All bone parameters were presented according to ASBMR guidelines [10].

In addition, commercially available ELISA for the bone resorption marker C-terminal telopeptide of type I collagen (CTX-I) and formation marker propeptide of type 1 procollagen (P1NP) were performed according to the manufacturing protocols (IDS, Frankfurt/Main, Germany). To measure the absorbance, the FLUOstar OMEGA was used and the results were evaluated with the associated analysis program.

Flow cytometry and cell sorting

Stromal subpopulations (MSPC, OBC, and EC) were sorted or analyzed as non-hematopoietic ($CD45^-$ $TER119^-$) cells as described [11, 12].

Stromal cell (MSPC) isolation and culture

Flushed long bones from mice were crushed and digested as described [9, 13]. Sorted MSPCs or MSPCs from digested compact bone were cultured on 0.1% gelatine-coated plates in MEM Alpha (with ribosides and Glutamax, Invitrogen), supplemented with fetal calf serum (FCS, 10%; PAA), antibiotics and 0,1% β-mercapto-ethanol (Invitrogen).

Fibroblast colony-forming units (CFU-F assay)

In order to evaluate the potential of MSPCs to develop colony-forming unit fibroblasts (CFU-Fs), 500 to 1000 sorted (p0) or cultured (p3) cells were plated in a well of a 6-well plate covered with 2 ml MSPC medium. After three days (cultured MSPCs) and ten days (sorted MSPCs), the colonies were counted under the microscope.

Assessment of DNA damage

Sorted LT-HSCs were tested upon nucleic acid damage by single cell gel electrophoresis (Comet Assay) from Cell Biolab. Therefore, LT-HCS were sorted out of two to three pools of mice per experiment. In the beginning, the Lysis Buffer, Alkaline Solution and the Electrophoresis Running Solution were prepared. The OxiSelect™Comet Agarose was heated to 90 °C for 20 min in a water bath and then cooled at 37 °C for 20 min. Afterwards, 75 µl of the Comet Agarose was added to the OxiSelect™Comet Slide to generate a base layer. After

15 min at 4 °C, the suspension cells were prepared with a total of 1 x 10^5cells/ml. The cells and the Comet Agarose were mixed in a 1:10 ratio and 75 µl of the mixture was spotted onto the top of the base layer. After an incubation of 15 min at 4 °C in the dark, an alkaline electrophoresis was performed for 30 min at 1 volt/cm. Immediately, the slides were washed three times in cold H2O for 2 min and one time in cold 70% ethanol for 5 min. The ethanol was removed by air-drying the slide, followed by adding 100 µl/well of diluted Vista Green DNA Dye (1:10,000 in TE Buffer). After 15 min of incubation at room temperature, fluorescence images were recorded with constant settings on a Leica DM RBE fluorescent microscope (AxioVision software; Carl Zeiss). For each genotype and each condition, 30 - 40 random cells were recorded at 100-fold magnification. The DNA damage of the cells was then analyzed by measuring the shift between the comet head (nucleus) and the resulting tail (DNA damage).

Single cell culture (SCC assay)

LT-HSCs were sorted into the inner 60 wells of a round-bottomed 96-well plate preloaded with 100 µl of 0.25 nm filtered conditioned media (CM) and supplemented with two growth factors: rmSCF (100 ng/ml) and/or rmIL-11 (20 ng/ml), additionally in some experiments supplemented with Collagen I (300 µg/ml) and nerve growth factor (NGF, 250 ng/ml). Immediately after sorting, the round-bottomed 96-well plates were centrifuged for 5 min at 200*g* and microscopically inspected for the presence of single cells. Every 24 h each well was inspected and cells were counted for clonal growth. After 5 days, the number of clone sizes was determined. The cells that had divided at least once (> 2 cells/well) were harvested and stained with antibodies for lineage markers, KIT and SCA-1. The cells were analyzed on a CyAn ADP Lx P8 and evaluated with FlowJo software (TreeStar; FlowJo 8.8.6).

Analysis of immunofluorescent labeled cells

To determine total protein content, the number of pixels per cell was assessed using ImageJ software (v1.52). Pictures within one experiment were taken under standardized conditions (light intensity, exposure, diaphragm).

For mean fluorescence intensity, the average intensity of pixels per cell was determined.

For foci analysis, the contrasts were visible by black and white processing within the digital images (Affinity Photo, Serif Europe Ltd). After threshold setting, cell structures were selected and counted automatically using ImageJ software.

Colocalization was assessed using ImageJ after picture processing by selection of single cells, background subtraction with the rolling ball algorithm, and threshold adjustment by the autothresholding method “Moment”. The ImageJ “Colocalization" plugin was then used to recover the overlapping pixels of two analysed proteins. The pixel area occupied were then collected by using the “Analyse particles” function. To identify colocalization bias either in nuclear proximity or the cytoplasm, the DAPI signal was used to delimit the nuclear area and the nuclear and cytoplasmic fractions were reported separately.

Senescence assay

Senescence was detected by using Senescence β-Galactosidase Staining Kit (Cell Signaling Technology). Sorted MSPCs (p1) or MSPCs from the bone chips (p4) were cultured for one week without medium change. The staining of the cellular senescence was performed following the manufacturer’s recommendation. In brief, the cells were washed twice with 1 ml 1 x DPBS and fixed for 6 to 7 min at room temperature using 1.5 ml 1 x Fixation Buffer. Meanwhile the staining mixture was prepared. The cells were washed with 1 x DPBS for three times, covered with 500 µl staining mixture per well and incubated overnight at 37 °C without

CO_2 to ensure a pH 6. The cells were analyzed by calculating the percentage of blue stained cells expressing β-galactosidase (senescent cells) against the non-blue (not senescent cells) under an Axiovert 25 microscope and an AxioVision software (Carl Zeiss).

RNA library preparation and sequencing

For the RNA sequencing (RNAseq) 800 to 1000 LT-HSCs were sorted in a well of a 96-well PCR plate (Eppendorf), prefilled with 5 µl 1 x TCL buffer (Qiagen) containing 1:100 β-mercaptoethanol. After sorting, the 96-well PCR plate was covered with aluminum foil for cold storage (VWR) and centrifuged for 1 min at 500 x *g*. Immediately after centrifugation, the cells were placed on dry ice and then stored at -80 °C until further usage.

The total RNA purification from the LT-HSCs and the reverse transcription into cDNA were performed as described previously [14].

The library preparation for bulk 3'-sequencing of poly(A)-RNA from niche cell populations was done as described previously [15]. Briefly, barcoded cDNA of each sample was generated with a Maxima RT polymerase (Thermo Fisher) using oligo-dT primer containing barcodes, unique molecular identifiers (UMIs) and an adapter. 5' ends of the cDNAs were extended by a template switch oligo (TSO). All samples were pooled, and the cDNA was amplified with primers binding to the TSO-site and the adapter. cDNA was tagmented with the Nextera XT kit (Illumina) and 3'-end-fragments finally amplified using primers with Illumina P5 and P7 overhangs. In comparison to Parekh et al. the P5 and P7 sites were exchanged to allow sequencing of the cDNA in read1 and barcodes and UMIs in read2 to achieve a better cluster recognition. The library was sequenced on a NextSeq 500 (Illumina) with 65 cycles for the cDNA in read1 and 16 cycles for the barcodes and UMIs in read2.

RNA sequencing data analysis

Gencode gene annotations M24 and the mouse reference genome GRCm38 were derived from the Gencode homepage (EMBL-EBI). Dropseq tools v1.12 [16] was used for mapping raw sequencing data to the reference genome. The resulting UMI filtered count matrix was imported into R v3.4.4.

Lowly expressed genes were filtered out prior to differential expression analysis with Limma [17]. Counts per Million (CPM) values were calculated (using the total number of reads per sample for scaling) and quantile normalized. The mean-variance trend was estimated with the limma function 'voomWithQualityWeights' where the genotype was used as explanatory variable. Moderated t-statistics were calculated for all possible pairwise comparisons (*Sfrp1*$^{fl/fl}$, OS1Δ/Δ, OS1Δ/Δ + IQ-1). A gene was determined to be significantly regulated if the adjusted p-value was below 0.05. Heatmap shows the z-scaled quantile-normalized expression values for genes being at least one time significantly regulated. Log2 fold changes were used for running GSEA [18] in the preranked mode with genesets from MSig DB v7.4 [18, 19]. A pathway was considered to be significantly associated with an experimental condition if the FWER was below 0.05.

Data and code availability

The published article includes all datasets generated or analyzed during this study. RNAseq data is available for download at ENA (European Nucleotide Archive) under the accession number PRJEB49216.

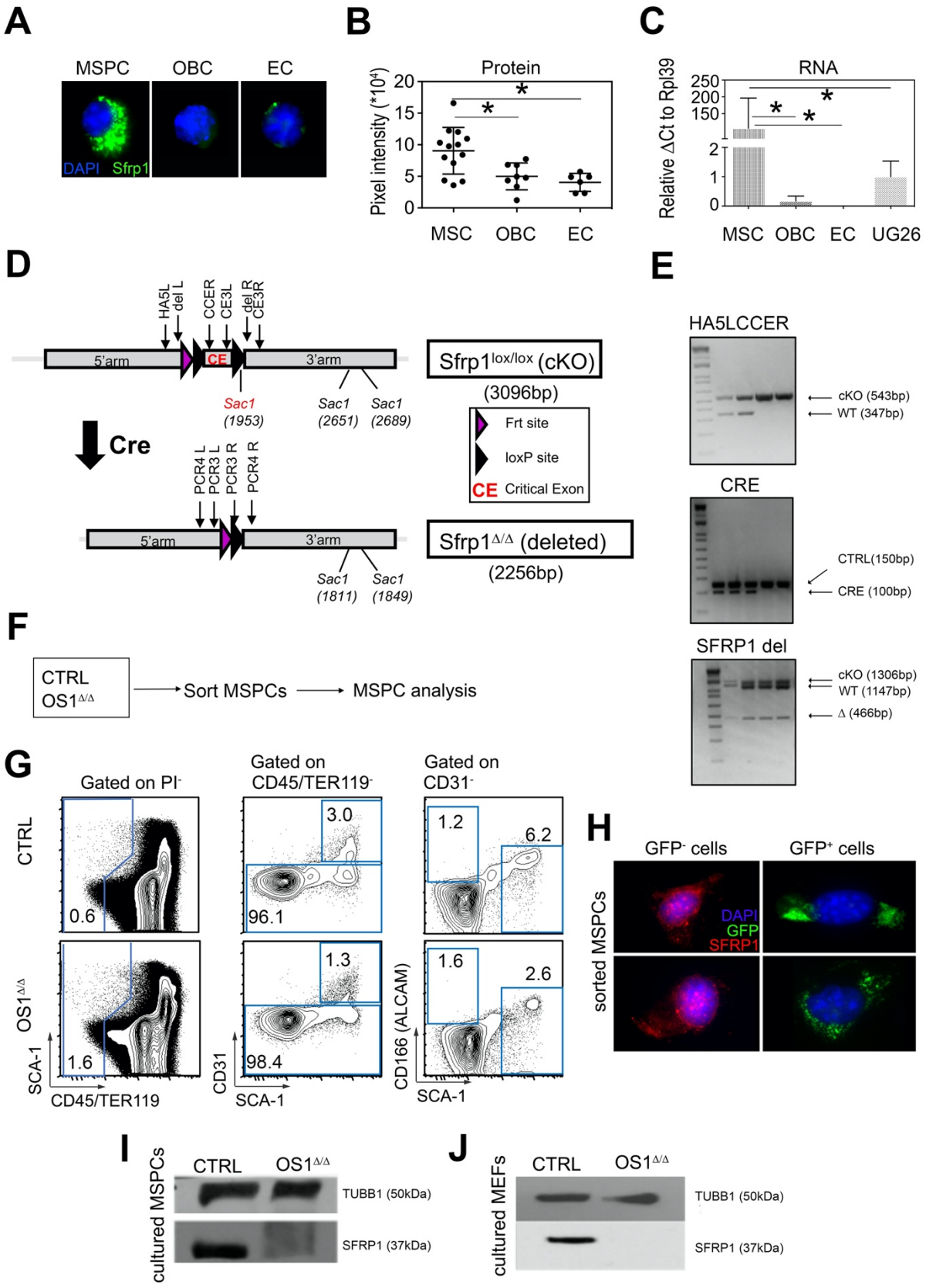

Figure S1. Generation and analysis of OS1Δ/Δ mice. A Representative picture of single-cell stains showing the expression of SFRP1 protein in stromal cell compartments. B Fluorescence pixel intensity measurements of SFRP1 in sorted MSPCs (n=13), OBCs (n=8) and ECs (n=6). C *Sfrp1* mRNA content

of sorted MSPCs (n=3), OBCs (n=3), ECs (n=3) and UG26-1B6 (n=3). The data represent the relative ΔCt value to the housekeeping gene *Rpl39*. D Generation and analysis of OS1Δ/Δ mice. In order to study Sfrp1 function we knocked out *Sfrp1* gene in stromal compartment by using newly generated *Sfrp1* conditional mouse crossed with mice expressing CRE and eGFP under the control of a tetO responsive Osx1 promotor. The used primer of the PCRs indicated in the scheme. E (Top) The expected PCR results (cKO 543bp; wt 347bp) are shown for the HA5L-CCER PCR. (Middle) The expected PCR results (internal control 150bp; CRE 100bp) are shown for the CRE PCR. (Bottom) The expected PCR results (cKO 1306bp; wt 1147bp; Δ 466bp) are shown for the *Sfrp1* del PCR. F Experimental design: MSPCs of 8 to 10 weeks-old OS1Δ/Δ mice and CTRL mice (*Sfrp1*$^{fl/fl}$) were sorted and analyzed. G Gating strategy for cell sorting of BM mesenchymal stem cell population. The mesenchymal stromal cells were gated as CD45^{-}Ter119^{-}CD31^{-}CD166^{-}SCA-1^{+} cells. H Representative fluorescence microscopy images of sorted MSPCs with the reporter IRES GFP as a selectable marker from CTRL (GFP^{-}) mice and OS1Δ/Δ (GFP^{+}) mice. I Western blot analysis of SFRP1 (37kDa) of CTRL and OS1Δ/Δ MSPCs. TUBB1 (50kDa) was used as a housekeeping gene. J Western blot analysis of SFRP1 (37kDa) of CTRL and OS1Δ/Δ MEFs. TUBB1 (50kDa) was used as a housekeeping gene. Each dot represents one cell (Figure S1B). Represented values are illustrated as Mean ± SD. *p-value ≤0.05 show significant differences determined by unpaired t test.

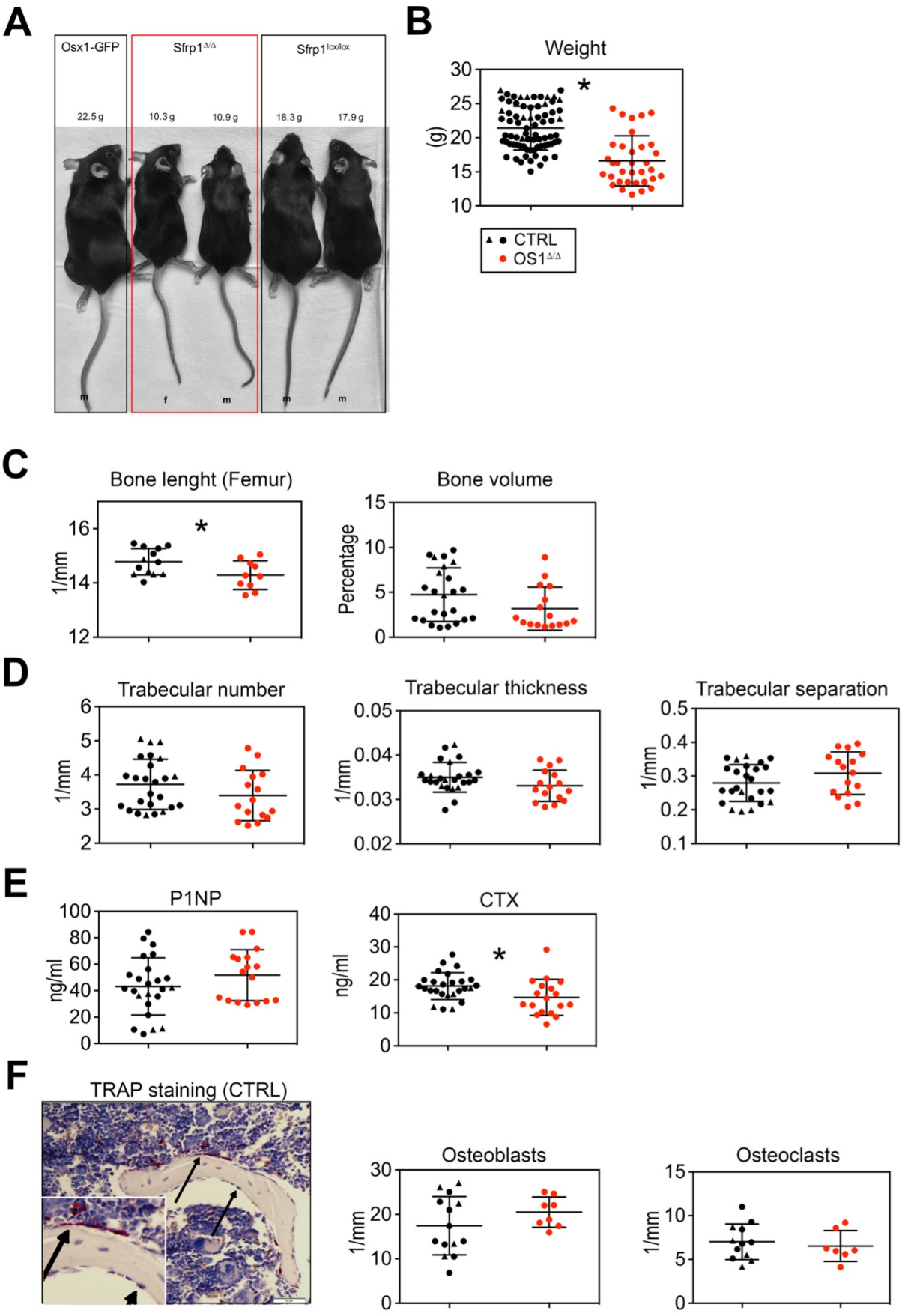
A
Osx1-GFP
Sfrp1Δ/Δ
Sfrp1lox/lox
22.5 g
10.3 g
10.9 g
18.3 g
17.9 g
m
f
m
m
m
B
Weight
(g)
30
25
20
15
10
*
CTRL
OS1Δ/Δ
C
Bone lenght (Femur)
1/mm
16
14
12
*
Bone volume
Percentage
15
10
5
0
D
Trabecular number
1/mm
6
5
4
3
2
Trabecular thickness
1/mm
0.05
0.04
0.03
0.02
Trabecular separation
1/mm
0.5
0.4
0.3
0.2
0.1
E
P1NP
ng/ml
100
80
60
40
20
0
CTX
ng/ml
40
30
20
10
0
*
F
TRAP staining (CTRL)
Osteoblasts
1/mm
30
20
10
0
Osteoclasts
1/mm
15
10
5
0

Figure S2. Characterization of the bone homeostasis in OS1Δ/Δ mice. A Representative picture of OS1Δ/Δ mice (n=2) and CTRL (n=3). C Decreased body weight of OS1Δ/Δ mice (n=34) compared to CTRL (n=75) in week 8. C Micro-computed tomography was used for the analysis of the trabecular bone from the femora of OS1Δ/Δ and CTRL. (Left) Femur length in OS1Δ/Δ (n=10) compared to CTRL (n=13). (Right) Percentage of bone volume of the femur in OS1Δ/Δ (n=16) compared to CTRL (n=24). D (Left) Trabecular number, (Middle) thickness and (Right) separation in OS1Δ/Δ (n=16) compared to CTRL (n=25). E (Left) The functionality of osteoblasts (CTRL: n=24; OS1Δ/Δ: n=17) and (Right) osteoclasts (CTRL: n=26, OS1Δ/Δ: n=18) were measured in serum by ELISA. F (Left) Representative images of tartrate-resistant acid phosphatase–stained (TRAP-stained) vertebrae of 8-week-old CTRL are depicted using the CellSens program and Microscope Axio Imager M1 (Carl Zeiss). In the TRAP-staining, osteoclasts are stained in red, while arrows indicate osteoblasts. Magnification: zoom of trabeculae 20× (scale bars: 50 µm). (Middle) Number of osteoblasts in OS1Δ/Δ (n=8) compared to CTRL (n=14) and (Right) osteoclasts in OS1Δ/Δ (n=7) compared to CTRL (n=12) per bone perimeter in femora. Each dot represents one animal (Figure B-F). Represented values are illustrated as Mean ± SD. *p-value ≤0.05 show significant differences determined by unpaired t test. Symbol legends as shown in Figure S2B. Black dots represent CTRL (*Sfrp1*$^{fl/fl}$). Black triangles represent CTRL (Osx-Cre).

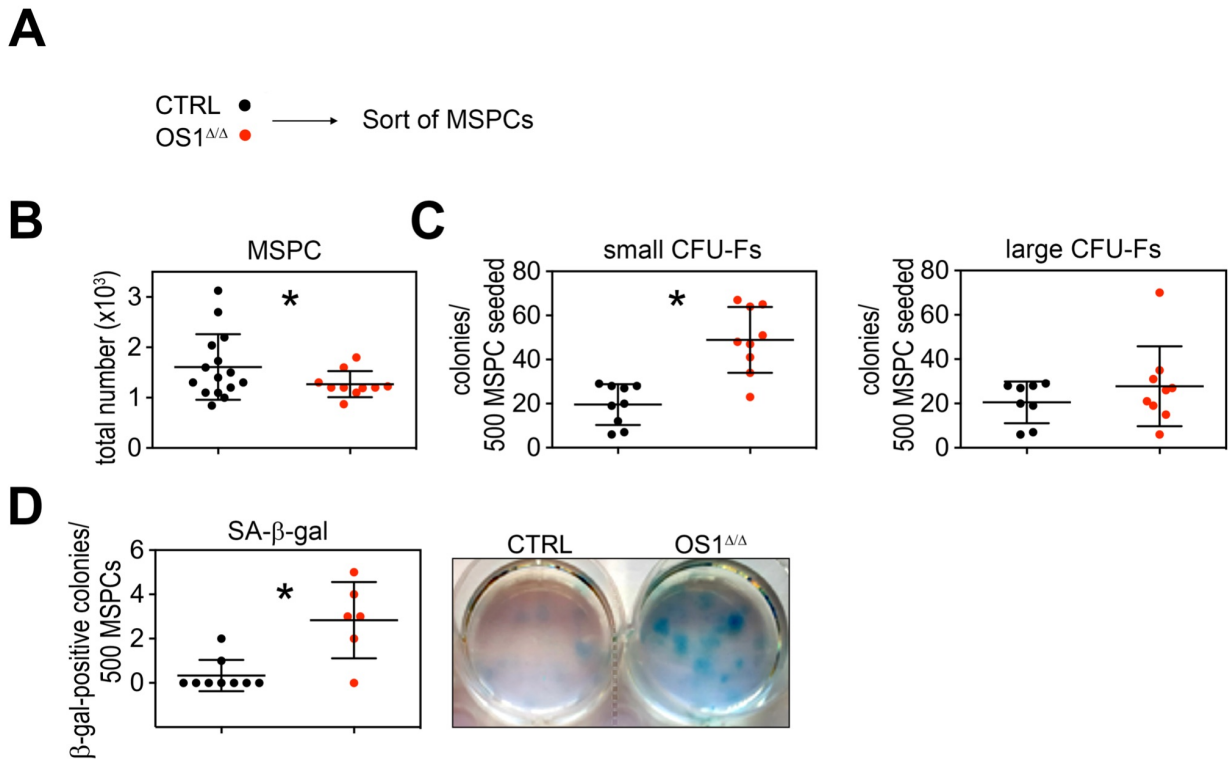

Figure S3. Analysis of MSPCs from CTRL mice and OS1Δ/Δ mice. A Experimental design: MSPCs of 8 to 10 weeks-old OS1Δ/Δ mice and CTRL mice (*Sfrp1*$^{fl/fl}$) were sorted and analyzed. B Total cell number of sorted MSPCs from OS1Δ/Δ mice (n=10) compared to CTRL (n=15). C 500 sorted MSPC seeded and total colonies counted after 10 days. (Left) Total number of small CFU-Fs (OS1Δ/Δ: n=9; CTRL: n=9; small <50 cells). (Right) Total number of large CFU-Fs (OS1Δ/Δ: n=8; CTRL: n=8; large >50cells). D (Left) Total number of SA-β-gal (blue stained) positive colonies of OS1Δ/Δ (n=6) compared to CTRL (n=9) per plate. (Right) Microscopy of SA-β-gal staining in OS1Δ/Δ MSPC colonies compared to CTRL. Each dot represents one animal (Figure B-D). Represented values are illustrated as Mean ± SD. *p-value ≤0.05 show significant differences determined by unpaired t test. Symbol legends as shown in Figure S3A.

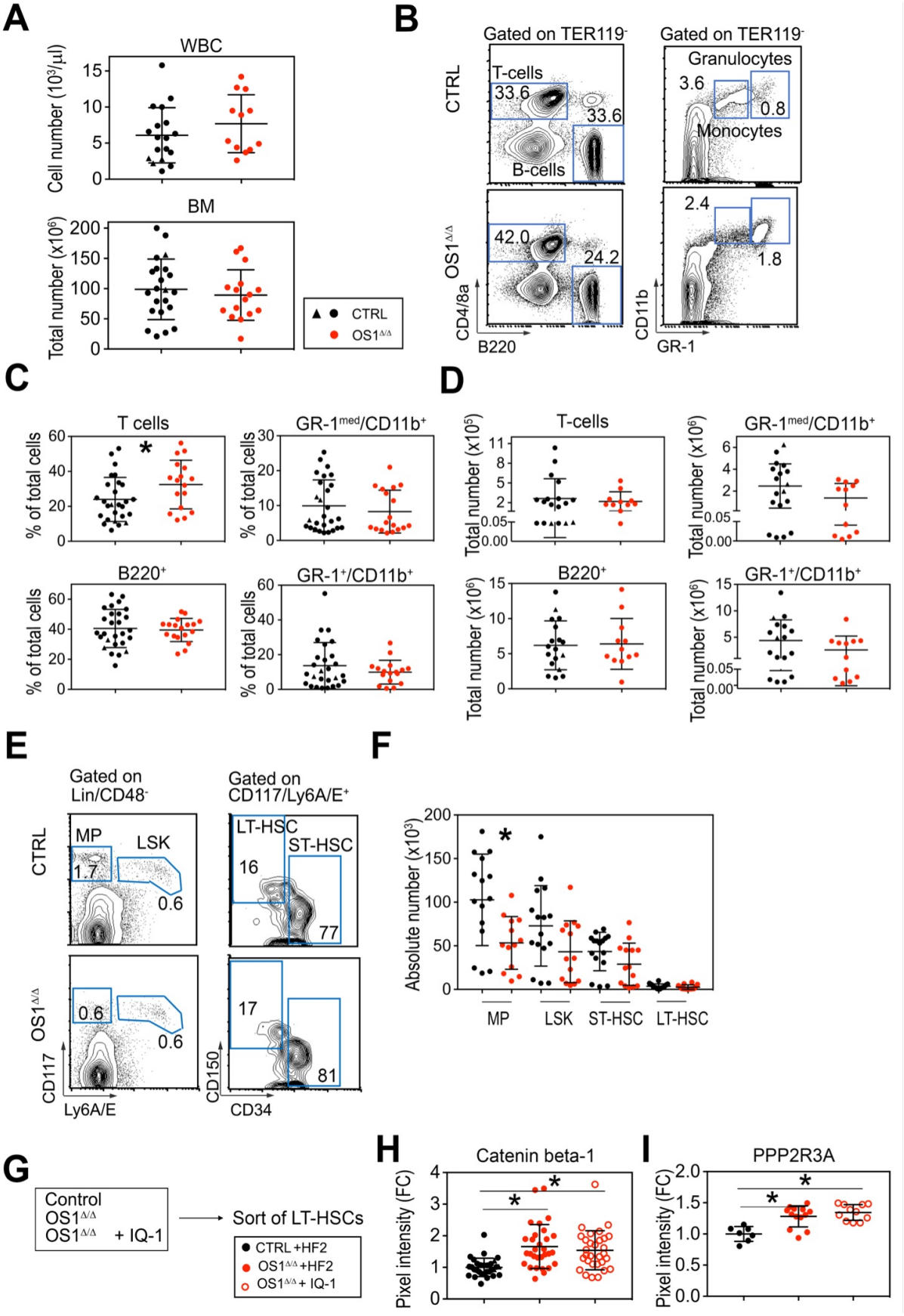

Figure S4. The influence on the mature and primitive hematopoietic compartment by *Sfrp1* loss in bone marrow niche cells. A (Top) Cell number of WBC of OS1Δ/Δ mice (n=12) compared to the CTRL (n=18). (Below) Total number of BM of OS1Δ/Δ mice (n=16) compared to CTRL (n=22). B Representative flow cytometry plots of the gating strategy for mature cell populations in PB. C **PB:** (Left,

top) Percentage of T cells, (Left, below) percentage of the $B220^+$ B cells, (Right, top) percentage of $GR1^{med}1CD11b^+$ monocytes, (Right, below) percentage of $GR1^+1CD11b^+$granulocytes of OS1Δ/Δ mice (n=18) compared to the CTRL (n=27). D **BM:** (Left, top) Absolute number of T cells, (Left, below) absolute number of the $B220^+$B cells, (Right, top) absolute number of $GR1^{med}CD11b^+$monocytes, (Right, below) absolute number of $GR1^+CD11b^+$granulocytes of OS1Δ/Δ mice (n=12) compared to the CTRL (n=17). E Representative flow cytometry plots of lineage depleted BM cells and the gating strategy for the primitive hematopoietic compartment. F Absolute number of MPs, LSKs, ST-HSCs and LT-HSCs of OS1Δ/Δ mice (n=14) compared to CTRL (n=16). G Experimental design: LT-HSCs of 8 to 10 weeks-old untreated and IQ1-treated OS1Δ/Δ mice and CTRL were sorted and analyzed per immunofluorescence for protein content of Catenin beta-1 and PPP2R3A. H Catenin beta-1 protein content as pixel number of LT-HSCs of OS1Δ/Δ mice (HF2: n=30; IQ-1: n =30) and CTRL (n=30). I PPP2R3A protein content as pixel number of LT-HSCs of OS1Δ/Δ mice (HF2: n=13; IQ-1: n =11) and CTRL (n=7). Each dot represents one animal (Figure A, C,D,F) or cell (Figure H,I). Represented values are illustrated as Mean ± SD. *p-value ≤0.05 show significant differences determined by unpaired t test. Symbol legends as shown in Figure S4F,G. Black dots represent CTRL (*Sfrp1*$^{fl/fl}$). Black triangles represent CTRL (Osx-Cre).

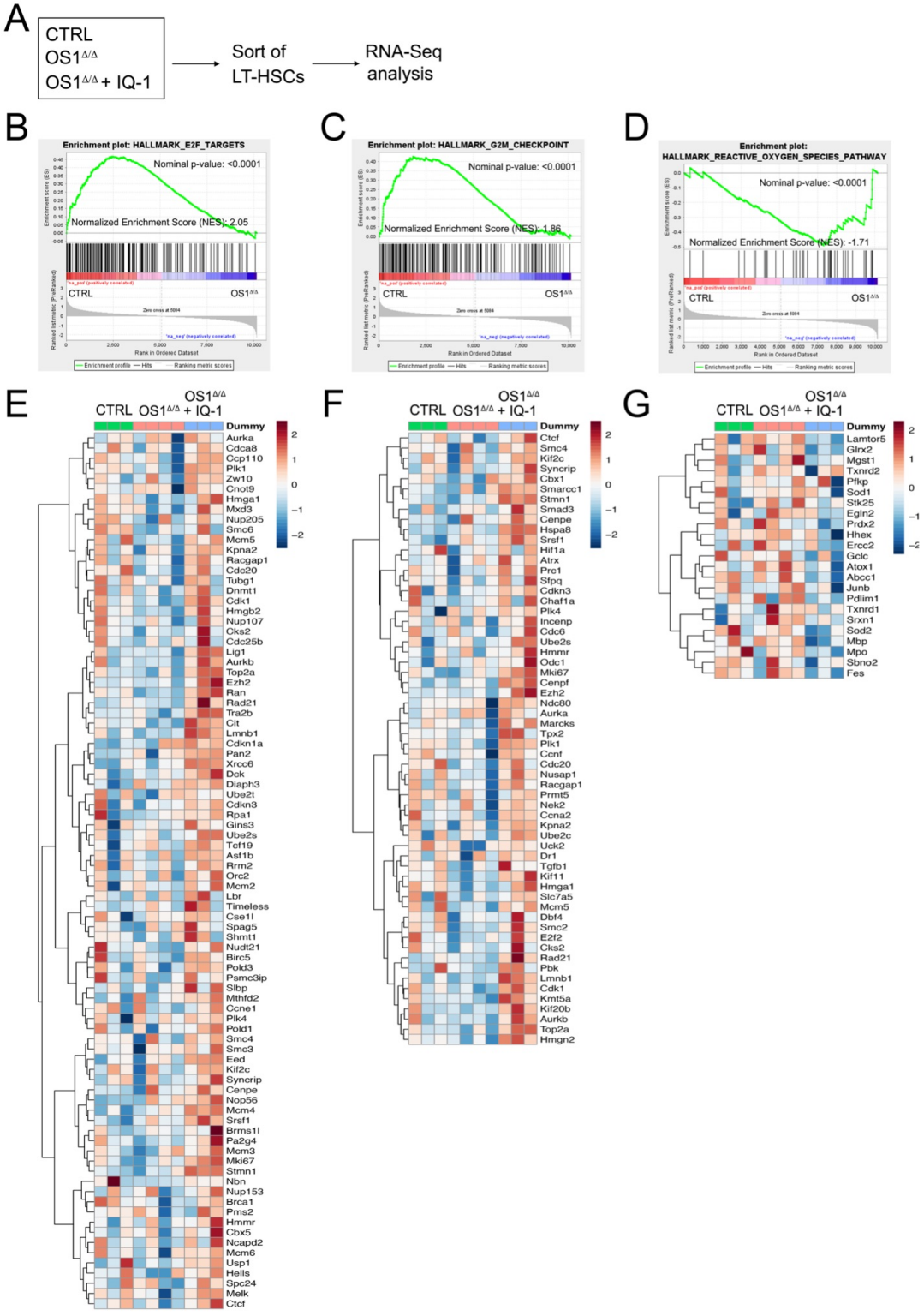

Figure S5. The cell cycle pathway is dysregulated in OS1Δ/Δ mice. A Experimental design: LT-HSCs of 8 to 10 weeks-old untreated and IQ-1-treated OS1Δ/Δ mice and CTRL (*Sfrp1*$^{fl/fl}$) were sorted and the transcriptomes were analyzed via RNAseq. B-D Gene Set Enrichment Analysis (GSEA) enrichment score curves of OS1Δ/Δ mice and CTRL. In each graph, red correlated with the most up-regulated genes and blue correlated with the most down-regulated genes. The green curve is the enrichment score (ES) curve. B Enrichment plot for Hallmark E2F targets. C Hallmark G2M checkpoint. D Hallmark reactive oxygen species pathway. E-G Heatmaps of DEGs in untreated and IQ-1-treated OS1Δ/Δ mice and CTRL. E Heatmap of DEGs: E2F targets. F Heatmap of DEGs: G2M checkpoint. G Heatmap of DEGs: reactive oxygen species pathway.

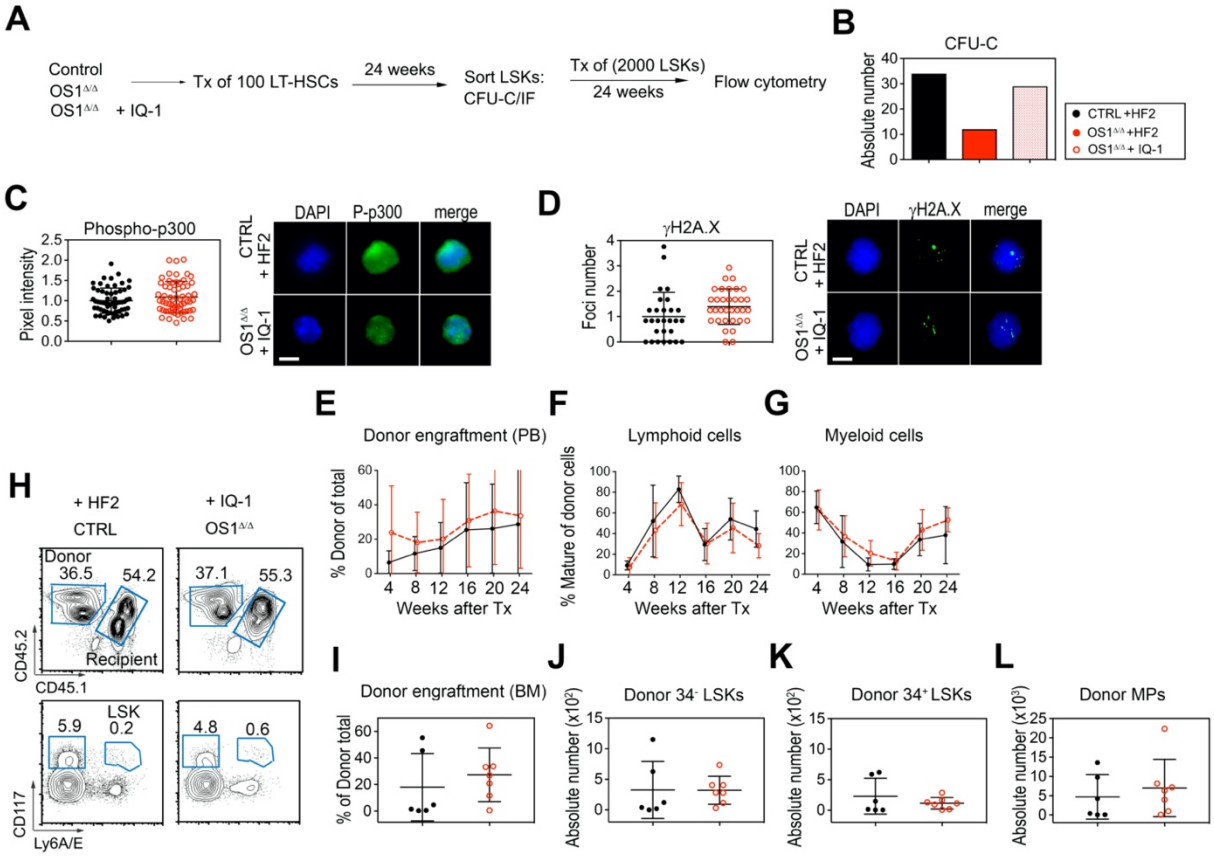

Figure S6. Cellular functions from primary Tx of IQ-1-treated and untreated CTRL mice and OS1Δ/Δ mice. A Experimental design of secondary Tx of IQ-1-treated LT-HSCs into lethally irradiated recipients. 8 to 10 weeks-old OS1Δ/Δ mice were i.p treated for 5 days with IQ-1 (14 µg) or the vehiculum (HF2). 24 h after the last treatment the LT-HSCs were sorted and transplanted into lethally irradiated WT recipients. 24 weeks after Tx, donor LSK cells were sorted and transplanted into lethally irradiated WT recipients. B Counted total numbers of CFCs from primary Tx of untreated and IQ1-treated OS1Δ/Δ mice and CTRL. C (Left) Phospho-p300 protein content as relative pixel number from LSK cells of IQ1-treated OS1Δ/Δ mice (n=61) and CTRL (n=61). (Right) Representative immunofluorescence staining for the nuclei staining with DAPI in blue (Left), phospho-p300 protein in green (Middle) and the merged picture (Right) of LSK cells from IQ1-treated OS1Δ/Δ mice and CTRL. D (Left) Relative histone γH2A.X foci content from LSK cells of IQ1-treated OS1Δ/Δ mice (n=33) and CTRL (n=28). (right) Representative immunofluorescence staining for the nuclei staining with DAPI in blue (Left), histone γH2A.X foci content in green (Middle) and the merged picture (Right) of LSK cells from IQ1-treated OS1Δ/Δ mice and CTRL. E Donor cell engraftment in percentage in PB up to 24 weeks after secondary Tx. F Lymphoid cell engraftment in percentage in PB up to 24 weeks after secondary Tx. G Myeloid cell engraftment in percentage in PB up to 24 weeks after secondary Tx. H Representative flow cytometry plots of the gating strategy of Ly5.2 donor cells or Ly5.1 Ly5.2 recipient cells. I Percentage of the donor engraftment in BM, J Absolute number of the donor CD34$^-$LSKs, K Absolute number of the donor CD34$^+$LSKs, L Absolute number of the donor MPs from OS1Δ/Δ mice (IQ-1: n=7) compared to CTRL (HF2: n=6). J Each dot represents one animal (Figure F-I) or a cell (Figure K, L). Represented values are illustrated as Mean ± SD. *p-value ≤0.05 show significant differences determined by unpaired t test. Symbol legends are shown in Figure S6B.

Supplemental videos (to Figure 6B)

Confocal 3D-Animation of LT-HSCs from OS1Δ/Δ and CTRL mice. LT-HSCs of eight to ten weeks-old OS1Δ/Δ and CTRL (Sfrp1fl/fl) mice were sorted and analyzed by immunofluorescence staining. Confocal microscopy pictures were taken on a Leica SP8 confocal microscope. Cells were stained for p300 protein (red), DAPI (blue) and colocalization with PPP2R3A (=PR72/130) (white) as described in the Methods section. 3D-animation was done using the Imaris software (9.9.0; Oxford Instruments).

Videos

Staining: red: p300; white: colocalization of p300 with PPP2R3A; blue: DAPI

	Treatment of mice	**File name**
Video 1	CTRL + HF2	CTRL+HF2_image17_20220413_SFRP1.mp4
Video 2	CTRL + IQ-1	CTRL+IQ1_image32_20220413_SFRP1.mp4
Video 3	OS1 Δ /Δ + HF2	DEL+HF2_image8_20220413_SFRP1.mp4
Video 4	OS1 Δ /Δ + IQ-1	DEL+IQ1_image27_20220413_SFRP1.mp4

Supplementary Table S1

Antibodies for flow cytometry (incl. cell sorting) and immunofluorescence		
CD45 Monoclonal Antibody (30-F11), FITC	eBioscience	Cat#11-0451-82; PRID: AB_465050
CD45 Monoclonal Antibody (30-F11), PE	eBioscience	Cat#12-0451-82; RRID: AB_465668
CD45 Monoclonal Antibody (30-F11), PE-Cyanine5.5	eBioscience	Cat#35-0451-82; RRID: AB_469718
CD45 Monoclonal Antibody (30-F11), PE-Cyanine7	eBioscience	Cat#25-0451-82; RRID: AB_2734986
CD45 Monoclonal Antibody (30-F11), APC	eBioscience	Cat#17-0451-82; RRID: AB_469392
CD45 Monoclonal Antibody (30-F11), APC-eFluor 780	eBioscience	Cat#47-0451-82; RRID: AB_1548781
CD45 Monoclonal Antibody (30-F11), Pacific Blue	Invitrogen	Cat#MCD4528; RRID: AB_10373710
CD3e Monoclonal Antibody (145-2C11), PE-Cyanine5.5	Invitrogen, eBioscience	Cat#35-0031-82;RRID: AB_11219266
TER-119 Monoclonal Antibody (TER119), PE	Invitrogen	Cat#MA5-17824; RRID: AB_2539207
CD45R (B220) Monoclonal Antibody (RA3-6B2), PE-Cyanine7	Invitrogen	Cat#25-0452-81; RRID: AB_469627
Ly-6G/Ly-6C Monoclonal Antibody (RB6-8C5), Pacific Blue	Invitrogen	Cat#RM3028; RRID: AB_10376182
CD11b Monoclonal Antibody (M1/70), APC-Cyanine7	Invitrogen	Cat#A15390; RRID: AB_2534404
CD45.1 Monoclonal Antibody (A20), FITC	Invitrogen, eBioscience	Cat#11-0453-82; RRID: AB_465058
CD45.2 Monoclonal Antibody (104), PE	Invitrogen, eBioscience	Cat#12-0454-81; RRID: AB_465678
CD45.2 Monoclonal Antibody (104), eFluor 450	Invitrogen, eBioscience	Cat#48-0454-82;RRID: AB_11042125
CD117 (c-Kit) Monoclonal Antibody (2B8), PE	Invitrogen, eBioscience	Cat#12-1171-82; RRID: AB_465813
CD34 Monoclonal Antibody (RAM34), FITC	Invitrogen, eBioscience	Cat#11-0341-81; RRID: AB_465021
CD34 Monoclonal Antibody (RAM34), eFluor 450	Invitrogen, eBioscience	Cat#48-0341-82; RRID: AB_2043837
CD150 Monoclonal Antibody (9D1), APC	Invitrogen, eBioscience	Cat#17-1501-63; RRID: AB_469440

Ly-6A/E (Sca-1) Monoclonal Antibody (D7), PE-Cyanine7	Invitrogen, eBioscience	Cat#25-5981-81; RRID: AB_469669
c-Kit Monoclonal Antibody (2B8), APC-Cyanine7	Invitrogen	Cat#A15423; RRID: AB_2534436
CD150 Monoclonal Antibody (9D1), PE	Invitrogen, eBioscience	Cat#12-1501-82; RRID: AB_465873
TER-119 Monoclonal Antibody (Ter119), PE-Cy5.5	Invitrogen, eBioscience	Cat#35-5921-82; PRID: AB_469738
CD31 (PECAM-1) Monoclonal Antibody (390), APC	Invitrogen, eBioscience	Cat#17-0311-82; RRID: AB_657735
CD166 (ALCAM) Monoclonal Antibody (eBioALC48), PE	Invitrogen, eBioscience	Cat#12-1661-81; RRID: AB_823125
TER-119 Monoclonal Antibody (TER119), Biotin	Invitrogen	Cat#MA5-17819; RRID: AB_2539203
CD48 Monoclonal Antibody (HM48-1), Biotin	Invitrogen, eBioscience	Cat#13-0481-82; RRID: AB_466470
CD11b Monoclonal Antibody (M1/70), Biotin	Invitrogen, eBioscience	Cat#13-0112-85; RRID: AB_466359
CD8a Monoclonal Antibody (53-6.7), Biotin	Invitrogen, eBioscience	Cat#13-0081-82; RRID: AB_466346
CD45R (B220) Monoclonal Antibody (RA3-6B2), Biotin	Invitrogen, eBioscience	Cat#13-0452-82; RRID: AB_466449
Ly-6G/Ly-6C Monoclonal Antibody (RB6-8C5), Biotin	Invitrogen, eBioscience	Cat#13-5931-86; RRID: AB_466802
Streptavidin eFluor™ 450 Conjugate	eBioscience	Cat#48-4317-82;RRID: AB_10359737
Streptavidin, APC-Alexa Fluor™ 750	Invitrogen	Cat#SA1027; RRID: AB_2716627
Anti-mouse CD150 (SLAM) Antibody (TC15-12F12.2), PE	BioLegend	Cat#115904; RRID: AB_313683
Anti-phospho-Histone H2A.X (Ser139) Antibody (JBW301); mouse	Sigma-Aldrich	Cat#05-636; PRID: AB_309864
Mouse Hematopoietic Lineage Biotin Panel	Invitrogen, eBioscience	Cat#88-7774-75; RRID: AB_476399
β-Catenin (L54E2) Mouse mAb	Cell Signaling Technologies	Cat#2677S
CBP (D6C5) Rabbit mAb	Cell Signaling Technologies	Cat#7389S
Anti-p300 CT Antibody, clone RW128	Upstate/ Millipore	Cat#05-257
Phospho-p300 (Ser89) Polyclonal Antibody	Invitrogen	Cat#PA5-12652

Phospho-β-Catenin (Ser33/37/Thr41) Antibody	Cell Signaling Technologies	Cat#9561
SFRP1 Antibody	Cell Signaling Technologies	Cat#4690
Rabbit anti-Goat IgG (H+L) Cross-Adsorbed Secondary Antibody, Alexa Fluor 488	eBioscience	Cat#A-11078; PRID: AB_2534122
Donkey anti-Goat IgG (H+L) Cross-Adsorbed Secondary Antibody, Alexa Fluor 594	Invitrogen	Cat#A-11058; PRID: AB_2534105
Goat anti-Mouse IgG (H+L) Cross-Adsorbed Secondary Antibody, Alexa Fluor 488	Invitrogen	Cat#A-11001; PRID: AB_2534069
Goat anti-Rabbit IgG (H+L) Cross-Adsorbed Secondary Antibody, Alexa Fluor 488	Invitrogen	Cat#A-11008; RRID: AB_143165
Goat anti-Mouse IgG (H+L) Cross-Adsorbed Secondary Antibody, Alexa Fluor 594	Invitrogen	Cat#A-11005; RRID: AB_2534073

Supplementary Tabe S2

Oligonucleotides for genotyng		
Sfrp1_Cond_F: GGAGTCCCTATGGCACTTCA	N/A	N/A
Sfrp1_Cond_R: AGCTGCTGTGAGTACCTGAA	N/A	N/A
OsterixCreTransgence_F: GAGAATAGGAACTTCGGAATAGTAAC	https://www.jax.org/strain/006361	N/A
OsterixCreTransgene_R: CCCTGGAAGTGACTAGCATTG	https://www.jax.org/strain/006361	N/A
OsterixCreInternControl_F: AGAGAGCTCCCCTCAATTATGT	https://www.jax.org/strain/006361	N/A
OsterixCreInternControl_R: AGCCACTTCTAGCACAAAGAACT	https://www.jax.org/strain/006361	N/A

Supplementary references

1. Pettitt SJ, Liang Q, Rairdan XY, et al. Agouti C57BL/6N embryonic stem cells for mouse genetic resources. Nat Methods. 2009;6(7):493-495.
2. Skarnes WC, Rosen B, West AP, et al. A conditional knockout resource for the genome-wide study of mouse gene function. Nature. 2011;474(7351):337-342.
3. Sadowski PD. The Flp recombinase of the 2-microns plasmid of Saccharomyces cerevisiae. Prog Nucleic Acid Res Mol Biol. 1995;51:53-91.
4. Rodda SJ, McMahon AP. Distinct roles for Hedgehog and canonical Wnt signaling in specification, differentiation and maintenance of osteoblast progenitors. Development. 2006;133(16):3231-3244.
5. Mizoguchi T, Pinho S, Ahmed J, et al. Osterix marks distinct waves of primitive and definitive stromal progenitors during bone marrow development. Dev Cell. 2014;29(3):340-349.
6. Chen J, Shi Y, Regan J, et al. Osx-Cre targets multiple cell types besides osteoblast lineage in postnatal mice. PLoS One. 2014;9(1):e85161.
7. Marquez SR, Hettler F, Hausinger R, et al. Secreted factors from mouse embryonic fibroblasts maintain repopulating function of single cultured hematopoietic stem cells. Haematologica. 2021;106(10):2633-2640.
8. Renström J, Istvanffy R, Gauthier K, et al. Secreted frizzled-related protein 1 extrinsically regulates cycling activity and maintenance of hematopoietic stem cells. Cell Stem Cell. 2009;5(2):157-167.
9. Schreck C, Istvanffy R, Ziegenhain C, et al. Niche WNT5A regulates the actin cytoskeleton during regeneration of hematopoietic stem cells. J Exp Med. 2017;214(1):165-181.
10. Dempster DW, Compston JE, Drezner MK, et al. Standardized nomenclature, symbols, and units for bone histomorphometry: a 2012 update of the report of the ASBMR Histomorphometry Nomenclature Committee. J Bone Miner Res. 2013;28(1):2-17.
11. Zhu H, Guo ZK, Jiang XX, et al. A protocol for isolation and culture of mesenchymal stem cells from mouse compact bone. Nat Protoc. 2010;5(3):550-560.
12. Nakamura Y, Arai F, Iwasaki H, et al. Isolation and characterization of endosteal niche cell populations that regulate hematopoietic stem cells. Blood. 2010;116(9):1422-1432.
13. Landspersky T, Sacma M, Riviere J, et al. Autophagy in mesenchymal progenitors protects mice against bone marrow failure after severe intermittent stress. Blood. 2022;139(5):690-703.
14. Picelli S, Bjorklund AK, Faridani OR, et al. Smart-seq2 for sensitive full-length transcriptome profiling in single cells. Nat Methods. 2013;10(11):1096-1098.
15. Parekh S, Ziegenhain C, Vieth B, Enard W, Hellmann I. The impact of amplification on differential expression analyses by RNA-seq. Sci Rep. 2016;6:25533.
16. Macosko EZ, Basu A, Satija R, et al. Highly Parallel Genome-wide Expression Profiling of Individual Cells Using Nanoliter Droplets. Cell. 2015;161(5):1202-1214.
17. Ritchie ME, Phipson B, Wu D, et al. limma powers differential expression analyses for RNA-sequencing and microarray studies. Nucleic Acids Res. 2015;43(7):e47.
18. Subramanian A, Tamayo P, Mootha VK, et al. Gene set enrichment analysis: a knowledge-based approach for interpreting genome-wide expression profiles. Proc Natl Acad Sci U S A. 2005;102(43):15545-15550.
19. Liberzon A, Subramanian A, Pinchback R, et al. Molecular signatures database (MSigDB) 3.0. Bioinformatics. 2011;27(12):1739-1740.